

Capillary effect on water table fluctuations in unconfined aquifers

Jun Kong,¹ Cheng-Ji Shen,² Pei Xin,² Zhiyao Song,³ Ling Li,^{1,2} D. A. Barry,⁴ D.-S. Jeng,^{1,5} F. Stagnitti,⁶ D. A. Lockington,² and J.-Y. Parlange⁷

Received 26 December 2012; revised 19 March 2013; accepted 1 April 2013; published 28 May 2013.

[1] Parlange and Brutsaert (1987) derived a modified Boussinesq equation to account for the capillary effect on water table dynamics in unconfined aquifers. Barry et al. (1996) solved this equation subject to a periodic boundary condition. Their solution shows significant influence of capillarity on water table fluctuations, which evolve to finite-amplitude standing waves at the high frequency limit. Here we propose a new governing equation for the water table, which considers both horizontal and vertical flows in an unsaturated zone of finite thickness. An approximate analytical solution for periodic water table fluctuations based on the new equation was derived. In agreement with previous results, the analytical solution shows that the unsaturated zone's storage capacity permits water table fluctuations to propagate more readily than predicted by the Boussinesq equation. Furthermore, the new solution reveals a capping effect of the unsaturated zone on both the amplitude and phase of the water table fluctuations as well as the water table overheight. Due to the finite thickness of the unsaturated zone, the capillary effect on water table fluctuations is modified mainly with reduced amplitude damping and phase shift.

Citation: Kong, J., C.-J. Shen, P. Xin, Z. Song, L. Li, D. A. Barry, D.-S. Jeng, F. Stagnitti, D. A. Lockington, and J.-Y. Parlange (2013), Capillary effect on water table fluctuations in unconfined aquifers, *Water Resour. Res.*, 49, 3064–3069, doi:10.1002/wrcr.20237.

1. Introduction

[2] Oceanic oscillations produce water table fluctuations in coastal unconfined aquifers. As they propagate inland, the water table fluctuations are attenuated with increasing time lags. These fluctuations, representing basic characteristics of coastal groundwater, provide important information for understanding the properties and behavior of coastal aquifers, and have been subjected to numerous investigations [e.g., Parlange et al., 1984; Nielsen et al., 1997; Jiao and Tang, 1999; Li et al., 2000a; Li and Jiao, 2003; Jeng et al., 2005].

Although most previous research has been focused on tide-induced low-frequency water table dynamics [e.g., Nielsen, 1990; Li et al., 2000b, 2000c; Jeng et al., 2002], high-frequency water table fluctuations due to waves have also been studied [Li et al., 1997].

[3] Traditionally, models of water table fluctuations are based on the Boussinesq equation, which predicts increasing rates of amplitude damping with the frequency of the oceanic oscillations [e.g., Parlange et al., 1984; Nielsen, 1990]. According to these models, high-frequency waves would not induce water table fluctuations in coastal unconfined aquifers to any considerable distance inland, a result inconsistent with field observations. Li et al. [1997] found that consideration of capillarity explains the transmission of high-frequency water table fluctuations in coastal aquifers.

[4] Parlange and Brutsaert [1987] examined the capillary effect on water table dynamics. As the water table fluctuates, the pressure distribution above the water table varies, resulting in local water exchange across the water table. Parlange and Brutsaert [1987] modified the Boussinesq equation with an additional term to account for this mass transfer process. Barry et al. [1996] combined the approaches of Parlange et al. [1984] and Parlange and Brutsaert [1987]. They obtained and applied a depth-integrated model with capillarity incorporated to study the propagation of small-amplitude oscillations in an unconfined aquifer and derived an approximate analytical solution. Their results showed that the damping rate of the water table fluctuations reaches an asymptotic finite value as the forcing frequency on the boundary increases. In other words, damping effects on high-frequency water table fluctuations are bounded. Under the influence of capillarity,

Additional supporting information may be found in the online version of this article.

¹State Key Laboratory for Hydrology-Water Resources and Hydraulic Engineering, Hohai University, Nanjing, China.

²National Center for Groundwater Research and Training, School of Civil Engineering, The University of Queensland, Queensland, Australia.

³Key Laboratory of Virtual Geographic Environment under Ministry of Education, Nanjing Normal University, Nanjing, China.

⁴Laboratoire de technologie écologique, Institut d'ingénierie de l'environnement, Faculté de l'environnement naturel, architectural et construit (ENAC), Ecole polytechnique fédérale de Lausanne (EPFL), Lausanne, Switzerland.

⁵Griffith School of Engineering, Griffith University, Gold Coast Campus, Gold Coast, Australia.

⁶Research & Graduate Studies Office, University of Ballarat, Ballarat, Victoria, Australia.

⁷Department of Biological and Environmental Engineering, Cornell University, Ithaca, New York, USA.

Corresponding author: L. Li, National Center for Groundwater Research and Training, School of Civil Engineering, The University of Queensland, Queensland 4072, Australia. (l.li@uq.edu.au)

high-frequency waves can be transmitted into the aquifer over a considerable distance, as observed in the field. Moreover, the analytical solution of Barry *et al.* [1996] predicts that at the high-frequency limit, water table fluctuations become standing waves, also consistent with field observations [Li *et al.*, 1997]. This solution was further extended to a higher order by Jeng *et al.* [2005]. It should be noted that the capillary effect on water table dynamics has implications for a range of processes and phenomena in unconfined aquifers, for example, pumping tests [e.g., Moench, 2008]

[5] Despite the progress in the theoretical development, laboratory experiments have shown that the modified Boussinesq equation with the capillarity correction and other approximations for vertical flow effects still cannot describe fully the water table behavior under the influence of boundary oscillations [e.g., Cartwright *et al.*, 2003]. Our goal here is to extend the previous work to improve the water table dynamics model. The modified Boussinesq equation of Parlange and Brutsaert [1987] considered local water exchange across the water table assuming only vertical flow in the unsaturated zone. This same assumption was used by Barry *et al.* [1996]. In this work, both horizontal and vertical flows are incorporated. The new approach also takes into account the (finite) thickness of the unsaturated zone.

2. Theory

[6] As shown in Figure 1, we consider the water table fluctuations in a rectangular unconfined aquifer subjected to the influence of head oscillation at a side boundary ($x = 0$). The coordinate system and various physical quantities (parameters) are defined in the figure. The flow in the saturated and unsaturated zones underlying the water table behavior is described by Richards' equation [Richards, 1931],

$$\frac{\partial \theta}{\partial t} = \frac{\partial}{\partial x} \left[K(\psi) \frac{\partial \Phi}{\partial x} \right] + \frac{\partial}{\partial z} \left[K(\psi) \frac{\partial \Phi}{\partial z} \right], \tag{1}$$

where θ [L] is the soil water content, $\Phi = \psi + z$ [L] is the hydraulic head, ψ is the pressure head, z [L] is the elevation and $K(\psi)$ [LT^{-1}] is the hydraulic conductivity. The model of Gardner [1958] is used to describe θ and K as functions of ψ , i.e.,

$$\theta = (\theta_s - \theta_r) \exp(\alpha\psi) + \theta_r \quad \text{for } \psi < 0, \tag{2a}$$

$$\theta = \theta_s \quad \text{for } \psi \geq 0, \tag{2b}$$

and

$$K(\psi) = K_s \exp(\alpha\psi) \quad \text{for } \psi < 0, \tag{3a}$$

$$K(\psi) = K_s \quad \text{for } \psi \geq 0, \tag{3b}$$

where K_s [LT^{-1}] is the saturated hydraulic conductivity (assumed to be uniform and isotropic); α [L^{-1}] is related to the capillary rise length scale inversely; θ_s and θ_r [-] are the saturated and residual water content, respectively; and $n_e = \theta_s - \theta_r$ is the effective porosity [-].

2.1. Approximation Under the Hydrostatic Pressure Assumption

[7] Under the assumption of hydrostatic pressure, the hydraulic head (Φ) is constant in the vertical direction and

$$\Phi = h, \tag{4}$$

where h is the water table elevation [L]. The pressure head in the unsaturated zone is given by

$$\psi = h - z. \tag{5}$$

[8] Integrating equation (1) with respect to z from the impermeable base ($z = 0$) to the surface ($z = Z_0$) gives,

$$\int_0^{Z_0} \frac{\partial \theta}{\partial t} dz = \int_0^{Z_0} \frac{\partial}{\partial x} \left[K(\psi) \frac{\partial \Phi}{\partial x} \right] dz, \tag{6}$$

where the no (vertical) flow boundary condition has been applied at both the base and surface. The left-hand side of equation (6) can be evaluated as follows,

$$\begin{aligned} \int_0^{Z_0} \frac{\partial \theta}{\partial t} dz &= -n_e \exp[\alpha(h - Z_0)] \frac{\partial(h - Z_0)}{\partial t} + n_e \frac{\partial h}{\partial t} \\ &\quad - n_e \exp[\alpha(h - Z_0)] \frac{\partial Z_0}{\partial t} \\ &= n_e \{ 1 - \exp[\alpha(h - Z_0)] \} \frac{\partial h}{\partial t}. \end{aligned} \tag{7}$$

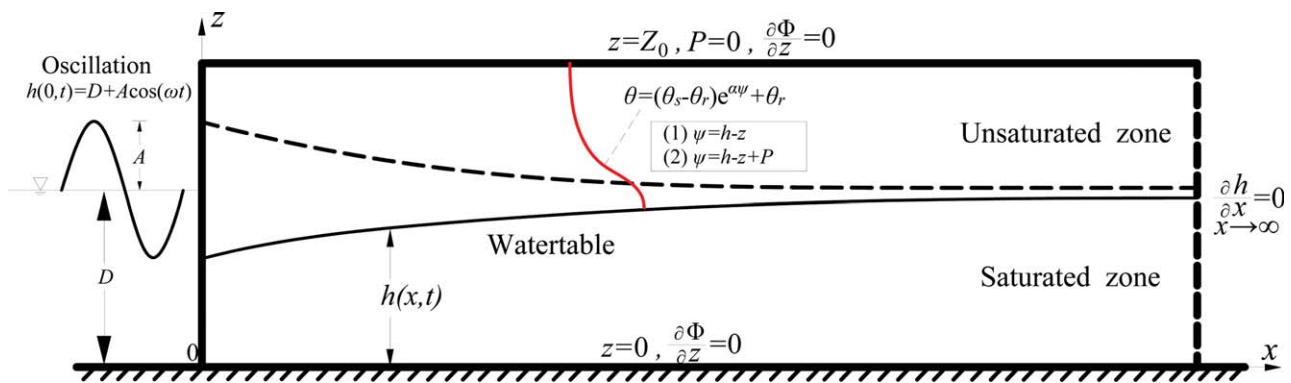


Figure 1. Schematic diagram of water table fluctuations in a rectangular unconfined aquifer under the influence of a periodic boundary condition.

[9] Upon evaluation, the right hand side of equation (6) becomes,

$$\int_0^{Z_0} \frac{\partial}{\partial x} \left[K(\psi) \frac{\partial \Phi}{\partial x} \right] dz = K_s \frac{\partial}{\partial x} \left\{ h \frac{\partial h}{\partial x} + \frac{1}{\alpha} \frac{\partial h}{\partial x} - \frac{1}{\alpha} \exp[\alpha(h - Z_0)] \frac{\partial h}{\partial x} \right\}. \quad (8)$$

[10] Substituting equations (7) and (8) into equation (6) yields a new governing equation for the water table dynamics,

$$n_e \{1 - \exp[\alpha(h - Z_0)]\} \frac{\partial h}{\partial t} = K_s \frac{\partial}{\partial x} \left\{ h \frac{\partial h}{\partial x} + \frac{1}{\alpha} \frac{\partial h}{\partial x} - \frac{1}{\alpha} \exp[\alpha(h - Z_0)] \frac{\partial h}{\partial x} \right\}. \quad (9)$$

[11] Further details of the derivation can be found in the supplementary material. It can be shown that equation (9) reduces to the standard Boussinesq model [e.g., Bear, 1972] as $\alpha \rightarrow \infty$ (the case where the unsaturated zone is neglected).

2.2 Nonhydrostatic Pressure Correction

[12] A nonhydrostatic pressure correction can be made to equation (5), i.e.,

$$\psi = h - z + P, \quad (10)$$

where P is the dynamic pressure head [L] and depends on the vertical (Darcy) flow velocity (w) in the unsaturated zone, i.e.,

$$\frac{\partial P}{\partial z} = -\frac{w}{K}. \quad (11)$$

[13] Mass conservation requires (assuming no recharge)

$$\frac{\partial \theta}{\partial t} + \frac{\partial u}{\partial x} + \frac{\partial w}{\partial z} = 0, \quad (12)$$

where u is the horizontal (Darcy) flow velocity [L/T].

[14] Integrating equation (12) in the vertical direction from a location (z) within the unsaturated zone to the surface (Z_0) gives

$$\int_z^{Z_0} \frac{\partial \theta}{\partial t} dz + \int_z^{Z_0} \frac{\partial u}{\partial x} dz + \int_z^{Z_0} \frac{\partial w}{\partial z} dz = 0. \quad (13)$$

[15] With no (vertical) flow at Z_0 , equation (13) leads to

$$w = \int_z^{Z_0} \frac{\partial \theta}{\partial t} dz + \int_z^{Z_0} \frac{\partial u}{\partial x} dz, \quad (14a)$$

with

$$\int_z^{Z_0} \frac{\partial \theta}{\partial t} dz = n_e \frac{\partial h}{\partial t} \{ \exp[\alpha(h - z)] - \exp[\alpha(h - Z_0)] \}, \quad (14b)$$

$$\int_z^{Z_0} \frac{\partial u}{\partial x} dz = K_s \left[\left(\frac{\partial h}{\partial x} \right)^2 + \frac{1}{\alpha} \frac{\partial^2 h}{\partial x^2} \right] \{ \exp[\alpha(h - Z_0)] - \exp[\alpha(h - z)] \}. \quad (14c)$$

[16] Thus,

$$\frac{\partial P}{\partial z} = -\frac{w}{K} = \{ \exp[\alpha(z - Z_0)] - 1 \} \left[\frac{n_e}{K_s} \frac{\partial h}{\partial t} - \left(\frac{\partial h}{\partial x} \right)^2 - \frac{1}{\alpha} \frac{\partial^2 h}{\partial x^2} \right], \quad (15)$$

where it has been assumed that $K \approx K_s \exp[\alpha(h - z)]$ since the magnitude of P is generally small compared with that of $(h - z)$ and hence $\exp[\alpha(h - z + P)] \approx \exp[\alpha(h - z)]$ (i.e., negligible effect of P on K); and

$$P = -\int_z^{Z_0} \frac{\partial P}{\partial z} dz = \left[\frac{1}{\alpha} \frac{\partial^2 h}{\partial x^2} - \frac{n_e}{K_s} \frac{\partial h}{\partial t} + \left(\frac{\partial h}{\partial x} \right)^2 \right] \left\{ \frac{1}{\alpha} - \frac{1}{\alpha} \exp[\alpha(z - Z_0)] - Z_0 + z \right\}. \quad (16)$$

[17] P also varies with x , which leads to an additional term in equation (8):

$$\int_h^{Z_0} K_s \exp[\alpha(h - z)] \frac{\partial P}{\partial x} dz \approx \frac{n_e}{\alpha^2} \{ 2 \exp[\alpha(h - Z_0)] - 2 + \alpha(Z_0 - h) \exp[\alpha(h - Z_0)] + \alpha(Z_0 - h) \} \frac{\partial^2 h}{\partial x \partial t}. \quad (17)$$

[18] With this term added to the right hand side of equation (9), the new governing equation for the water table with a nonhydrostatic pressure correction is derived,

$$F n_e \frac{\partial h}{\partial t} = K_s \frac{\partial}{\partial x} \left(M h \frac{\partial h}{\partial x} \right) + \frac{\partial}{\partial x} \left(N \frac{\partial^2 h}{\partial x \partial t} \right), \quad (18a)$$

with

$$F = 1 - \exp[\alpha(h - Z_0)], \quad (18b)$$

$$M = 1 + \frac{1}{\alpha h} \{ 1 - \exp[\alpha(h - Z_0)] \}, \quad (18c)$$

$$N = \frac{n_e}{\alpha^2} \{ 2 \exp[\alpha(h - Z_0)] - 2 + \alpha(Z_0 - h) \exp[\alpha(h - Z_0)] + \alpha(Z_0 - h) \}. \quad (18d)$$

[19] F is positive and smaller than unity, reflecting a reduction in the effective void space for local water storage and leading to enhancement of water table fluctuations. M is larger than unity due to the horizontal flux in the unsaturated zone. N is the nonhydrostatic pressure correction term, which accounts for the effect of vertical flow in the unsaturated zone. To make a nonhydrostatic pressure correction for the saturated zone, the work of Parlange et al. [1984] and Liu and Wen [1997] can be adopted to include an additional term in N , i.e.,

$$N = \frac{n_e}{\alpha^2} \{ 2 \exp[\alpha(h - Z_0)] - 2 + \alpha(Z_0 - h) \exp[\alpha(h - Z_0)] + \alpha(Z_0 - h) \} + \frac{D^2 n_e}{3}, \quad (19)$$

where D is the average aquifer thickness.

3. Analytical Solution

[20] Using perturbation, we solved equation (18) subject to a periodic boundary condition for a semi-infinite aquifer domain (details in the supplementary material). The first-order approximation gives the following solution for the primary frequency (ω),

$$h = D + A \exp(-xk_{US} F_1) \cos(\omega t - xk_{US} F_2), \quad (20a)$$

with

$$k_{US} = \sqrt{\frac{R_1 \omega}{2R_2}}, \quad (20b)$$

$$N_{US} = \frac{R_2}{R_3 \omega}, \quad (20c)$$

$$F_1 = \sqrt{\frac{N_{US}}{\sqrt{1+N_{US}^2}} + \frac{N_{US}}{1+N_{US}^2}}, \quad (20d)$$

$$F_2 = \sqrt{\frac{N_{US}}{\sqrt{1+N_{US}^2}} - \frac{N_{US}}{1+N_{US}^2}}, \quad (20e)$$

$$R_1 = n_e \{1 - \exp[\alpha(D - Z_0)]\}, \quad (20f)$$

$$R_2 = K_s D + K_s \frac{1}{\alpha} \{1 - \exp[\alpha(D - Z_0)]\}, \quad (20g)$$

$$R_3 = \frac{n_e}{\alpha^2} \left\{ 2 \exp[\alpha(D - Z_0)] - 2 + \alpha(Z_0 - D) \exp[\alpha(D - Z_0)] + \alpha(Z_0 - D) + \frac{D^2 \alpha^2}{3} \right\}, \quad (20h)$$

where A is the amplitude of the hydraulic head oscillations at the boundary. When ω approaches infinity, $F_1 = 1$ and $F_2 = 0$, and water table fluctuations become standing waves. The second-order solution was also derived (supplementary material).

[21] To validate the approximate analytical solution, equation (18) was solved numerically. A harmonic analysis on the predicted water table fluctuations given by the numerical solution was conducted to determine the damping rate and wave number (phase shift) associated with the oscillations at the primary frequency (ω). Comparison of these results with the analytical predictions shows reasonably good agreement between the two (Figure 2). The results also display considerable variations in the damping rate and wave number with the thickness of the unsaturated zone (with Z_0 varying for fixed D). The variations are not monotonic – both parameters increase with Z_0 to a maximum followed by a gradual decline as described by equation (20).

3.1. Dispersion Relation

[22] The dispersion relation given by the new analytical solution was compared with those of previous solutions, based on the experimental case by *Cartwright et al.* [2003]. This relation characterizes the water table fluctuations and

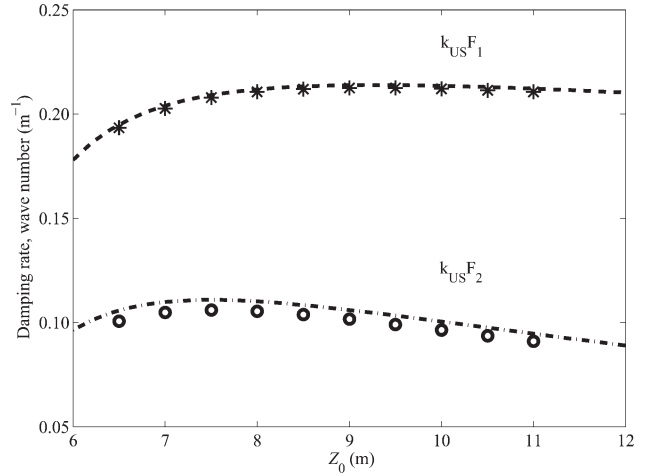


Figure 2. Comparison between the damping rate and wave number of the primary (ω) water table fluctuations given by the analytical and numerical solutions. Stars and circles are the numerical results of the damping rate and wave number, respectively. Dashed and dash-dotted lines are the analytical predictions of the damping rate and wave number (equation (20a)), respectively. Parameters values used were $A = 1$ m, $D = 5$ m, $\alpha = 1$ m $^{-1}$, $K_s = 0.00047$ m/s and $n_e = 0.3$.

can be expressed by a complex number (k) combining the damping rate (k_r) and wave number (k_i), i.e., $k = k_r + ik_i$.

[23] The solution for the water table fluctuations based on the traditional Boussinesq equation gives the following dispersion relation [*Parlange et al.*, 1984],

$$k = (1 + i) \sqrt{\frac{n_e \omega}{2DK_s}}, \quad (21)$$

where $k_r = k_i$. *Cartwright et al.* [2003] found $k_r/k_i \approx 2.3$ based on the results from their sand flume experiment. The condition $k_r/k_i > 1$ can be explained by the capillary effect and/or the vertical flow effect. For the former effect, *Barry et al.*'s [1996] solution gives,

$$k = \sqrt{\frac{n_e \omega}{2DK_s} \left[\frac{N_{CAR}}{\sqrt{1+N_{CAR}^2}} + \frac{N_{CAR}}{1+N_{CAR}^2} \right]} + \sqrt{\frac{n_e \omega}{2DK_s} \left[\frac{N_{CAR}}{\sqrt{1+N_{CAR}^2}} - \frac{N_{CAR}}{1+N_{CAR}^2} \right]} i, \quad (22a)$$

with

$$N_{CAR} = \frac{K_s}{B\omega}, \quad (22b)$$

where B is an equivalent capillary fringe thickness [*Parlange and Brutsaert*, 1987]. For the latter effect, *Nielsen et al.* [1997] suggested the following dispersion relation for medium-depth aquifers,

$$kD \tan kD = i \frac{n_e \omega D}{K_s}. \quad (23)$$

[24] A complex porosity (n_c) instead of n_e can be used in equation (23) to further incorporate the capillary effect [Cartwright *et al.*, 2003],

$$n_c = \frac{n_e}{1 + 2.5 \left(i \frac{n_e \omega H_e}{K_s} \right)^{2/3}}. \quad (24)$$

[25] Cartwright *et al.* [2003] found that neither equation (22) nor equation (23) described well the dispersion relation observed in data from their laboratory experiment (Figure 3). Direct application of the present solution with measured parameter values also failed to predict the observation; however, the data fell on the dispersion relation curve. With the saturated hydraulic conductivity adjusted from the measured value (0.00047 m/s) to 0.0008 m/s, the present solution predicted the experimental results. Considering the possible uncertainty associated with the K_s measurement, this adjustment by a factor less than two was relatively small, indicating the applicability of the dispersion relation given by the present solution.

3.2. Mean Water Table Elevation (Overheight)

[26] Oceanic oscillations induce not only water table fluctuations but also an overheight—i.e., the mean water table elevation far inland is higher than the mean water (head) level at the boundary [Knight, 1981]. The overheight increment (Δ), due to nonlinearity, is given by [e.g., Parlange *et al.*, 1984],

$$\Delta = D \left[\sqrt{1 + \frac{1}{2} \left(\frac{A}{D} \right)^2} \right] \approx D \left[1 + \frac{1}{4} \left(\frac{A}{D} \right)^2 \right]. \quad (25)$$

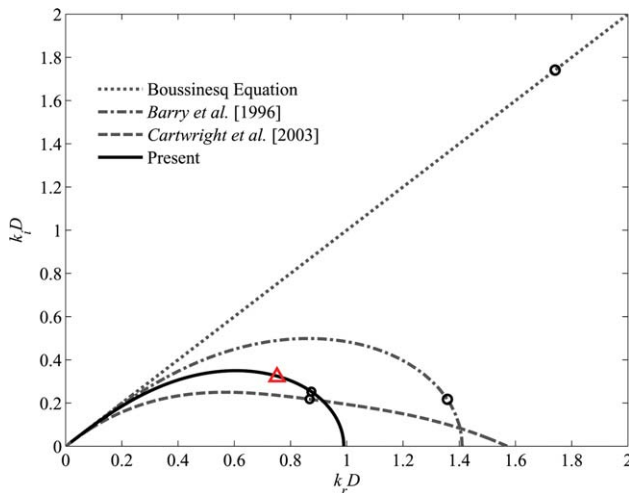


Figure 3. Comparison of amplitude damping rates $k_r D$ (real part of $k D$) and wave numbers $k_i D$ (for the primary frequency ω) given by different dispersion relation equations. The triangle denotes the measured value based on the experimental result. The circle on each curve indicates the calculated values based on measured parameter values and using the corresponding dispersion relation equation. The parameter values used were $T = 772$ s, $D = 1.094$ m, $n_e = 0.32$, $K_s = 0.00047$ m/s, $H_\psi = 0.55$ m and $\alpha = 1$ m⁻¹.

[27] Barry *et al.* [1996] found that the capillarity affects the time-averaged mean-square height of the water table. However, as the landward distance approaches infinity, their result reduces to equation (25). The present solution to second order as shown in the supplementary material also predicts the mean water table with an overheight,

$$H_{\text{OVER}} = D \left[1 + \frac{1}{4} N_{\text{OVER}} \left(\frac{A}{D} \right)^2 \right], \quad (26a)$$

with

$$N_{\text{OVER}} = \frac{R_4 F_1 - R_5 F_2 \omega}{R_2 F_1}, \quad (26b)$$

$$R_4 = K_s D \{ 1 - \exp[\alpha(D - Z_0)] \}, \quad (26c)$$

$$R_5 = \frac{n_e}{\alpha^2} \{ \exp[\alpha(D - Z_0)] \alpha D + \alpha^2 D (Z_0 - D) \exp[\alpha(D - Z_0)] - \alpha D \}, \quad (26d)$$

where the dimensionless number N_{OVER} is positive and mostly less than unity for the physical conditions considered, indicating the existence of a water table overheight but less than that predicted by equation (25). As ω increases, F_2 decreases and approaches zero and the overheight approaches $D \left[1 + \frac{1}{4} (A/D)^2 R_4/R_2 \right]$, which is still lower than the traditional overheight value for $0 < R_4/R_2 < 1$. As shown in Figure 4, N_{OVER} is affected by and increases with Z_0 until an asymptotic value is reached. This effect of finite unsaturated zone thickness is particularly strong for small α (strong capillarity).

4. Concluding Remarks

[28] Parlange and Brutsaert's [1987] work enabled investigation into the capillary effect on water table fluctuations in coastal unconfined aquifers induced by oceanic oscillations and has stimulated further studies in the area. In particular, their work provided an explanation for high-frequency water table fluctuations caused by waves.

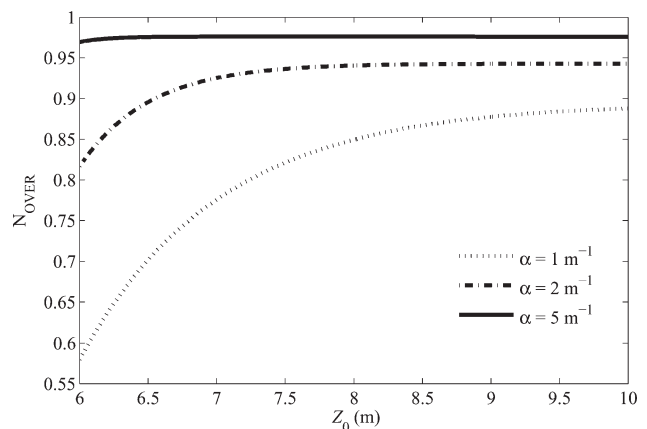


Figure 4. Variation of overheight index (N_{OVER}) with Z_0 for different α values ($K_s = 0.0005$ m/s, $D = 5$ m, $n_e = 0.3$ and $T = 12$ h).

[29] Here we have extended their approach to derive a new governing equation and analytical solution that incorporate both horizontal and vertical flows in governing the water table dynamics as well as the effect of the finite size of the unsaturated zone. These effects are shown to influence the dispersion relation of the water table fluctuations and the mean water table height. While the comparison with experimental data indicates improved predictions by the present solution compared with those given previously, further validation is required, particularly in relation to the effect of the finite unsaturated zone thickness. New experiments must be carried out under controlled conditions to provide comprehensive data sets for the validation. These experiments should include measurements of hydraulic heads (capillary pressure) in the unsaturated zone and tracer tests to track the water table dynamics and unsaturated flow near the water table.

[30] **Acknowledgments.** This work was supported by the National Basic Research Program of China (973 program, 2012CB417005), National Natural Science Foundation of China (51009059), National Science-Technology Support Program of China (2012BAB03B01) and Open Foundation of State Key Laboratory of Hydrology-Water Resources and Hydraulic Engineering (2011491311).

References

- Barry, D. A., S. J. Barry, and J.-Y. Parlange (1996), Capillarity correction to periodic solution of the shallow flow approximation, in *Mixing in Estuaries and Coastal Seas, Coastal Estuarine Stud.*, edited by C. B. Pattiaratchi, vol. 50, pp. 496–510, AGU, Washington, D. C.
- Bear, J. (1972), *Dynamics of Fluids in Porous Media*, Am. Elsevier Publ. Co., New York.
- Cartwright, N., P. Nielsen, and S. Dunn (2003), Water table waves in an unconfined aquifer: Experiments and modeling, *Water Resour. Res.*, 39(12), 1330, doi:10.1029/2003WR002185.
- Gardner, W. R. (1958), Some steady-state solutions of the unsaturated moisture flow equations with application to evaporation from a water table, *Soil Sci.*, 85(4), 228–232.
- Jeng, D.-S., L. Li, and D. A. Barry (2002), Analytical solution for tidal propagation in a coupled semi-confined/phreatic coastal aquifer, *Adv. Water Resour.*, 25(5), 577–584, doi:10.1016/S0309-1708(02)00016-7.
- Jeng, D.-S., B. R. Seymour, D. A. Barry, L. Li, and J.-Y. Parlange (2005), New approximation for free surface flow of groundwater: Capillarity correction, *Adv. Water Resour.*, 28(10), 1032–1039, doi:10.1016/j.advwatres.2004.05.012.
- Jiao, J. J., and Z. H. Tang (1999), An analytical solution of groundwater response to tidal fluctuation in a leaky confined aquifer, *Water Resour. Res.*, 35(3), 747–751, doi:10.1029/1998WR900075.
- Knight, J. H. (1981), Steady periodic-flow through a rectangular dam, *Water Resour. Res.*, 17(4), 1222–1224, doi:10.1029/WR017i004p01222.
- Li, H. L., and J. J. Jiao (2003), Tide-induced seawater-groundwater circulation in a multi-layered coastal leaky aquifer system, *J. Hydrol.*, 274(1–4), 211–224, doi:10.1016/S0022-1694(02)00413-4.
- Li, L., D. A. Barry, J.-Y. Parlange, and C. B. Pattiaratchi (1997), Beach water table fluctuation due to wave run-up: Capillarity effects, *Water Resour. Res.*, 33, 935–945, doi:10.1029/96WR03946.
- Li, L., D. A. Barry, C. Cunningham, F. Stagnitti, and J.-Y. Parlange (2000a), A two-dimensional analytical solution of groundwater responses to tidal loading in an estuary and ocean, *Adv. Water Resour.*, 23(8), 825–833, doi:10.1016/S0309-1708(00)00016-6.
- Li, L., D. A. Barry, F. Stagnitti, and J.-Y. Parlange (2000b), Groundwater waves in a coastal aquifer: A new governing equation including vertical effects and capillarity, *Water Resour. Res.*, 36(2), 411–420, doi:10.1029/1999WR900307.
- Li, L., D. A. Barry, F. Stagnitti, J.-Y. Parlange, and D.-S. Jeng (2000c), Beach water table fluctuations due to spring-neap tides: Moving boundary effects, *Adv. Water Resour.*, 23(8), 817–824, doi:10.1016/S0309-1708(00)00017-8.
- Liu, P. L.-F., and J. Wen (1997), Nonlinear diffusive surface waves in porous media, *J. Fluid Mech.*, 347, 119–139, doi:10.1017/S0022112097006472.
- Moench, A. F. (2008), Analytical and numerical analyses of an unconfined aquifer test considering unsaturated zone characteristics, *Water Resour. Res.*, 44, W06409, doi:10.1029/2006WR005736.
- Nielsen, P. (1990), Tidal dynamics of the water table in beaches, *Water Resour. Res.*, 26(9), 2127–2134, doi:10.1029/WR026i009p02127.
- Nielsen, P., A. M. Aseervatham, J. D. Fenton, and P. Perrochet (1997), Groundwater waves in aquifers of intermediate depths, *Adv. Water Resour.*, 20(1), 37–43, doi:10.1016/S0309-1708(96)00015-2.
- Parlange, J.-Y., and W. Brutsaert (1987), A capillarity correction for free surface flow of groundwater, *Water Resour. Res.*, 23(5), 805–808, doi:10.1029/WR023i005p00805.
- Parlange, J.-Y., F. Stagnitti, J. L. Starr, and R. D. Braddock (1984), Free-surface flow in porous media and periodic solution of the shallow-flow approximation, *J. Hydrol.*, 70(1–4), 251–263, doi:10.1016/0022-1694(84)90125-2.
- Richards, L. A. (1931), Capillary conduction of liquids in porous mediums, *Physics*, 1, 318–333, doi:10.1063/1.1745010.